An Application of Beam Dynamics to a Damper Design

Flexural wave propagation may be used as a means of absorbing impact energy to prevent excessive rebound or to shorten the cycle time of high-speed printing devices. For optimal damping action, however, the dynamic analysis of beams used in the mechanism is necessary; this paper presents such an analysis. It also presents an application of a damper ring design that is used to prevent so-called "shadow printing" by suppressing the rebound of the type elements in a disk printer.

Introduction

In many high-speed printing devices, the settle-out time of fast-moving components often plays an important role in limiting the repetition rate. Also, uncontrolled rebound of key components can result in mechanical interferences. This is particularly true in many impact printers used in computer systems. These printers invariably contain fast-moving type elements and hammers that must be settled out after each stroke before the next cycle can be initiated. Not only does a slow settle-out mean a slow cycle rate, but if these high-energy elements rebound excessively, they can cause double imprints or so-called "shadow printing."

The most common method of absorbing impact energy is to use some type of damping material. This approach is acceptable only if such material can be incorporated into the structure without affecting the operational performance. Another mechanism of energy absorption, while not commonly designed into a damper but which indirectly affects settle-out, is elastic or shock waves that propagate through the structure. If the structure is properly designed, a wave propagation can be successfully used as a means of energy dissipation. Compared to elastomers and polymers, however, elastic dampers usually require more careful analysis because wave propagation phenomena are more complex and sensitive to parameter variations.

One such damper design that uses flexural wave propagation is incorporated into the IBM 3610 disk printer [1]. Figure 1 shows the print-disk assembly, which contains the type and interposer disks pressed together. The type disk carries an array of type elements mounted on individual fingers that are very flexible in an out-of-plane direction. The interposer disk has thicker and stiffer fingers on which the individual type rests with some preload. The entire disk assembly rotates at very high speed (the peripheral speed is about 8 m/s). The hammer, poised for the right type character to come by, strikes the interposer at the right moment, transferring the momentum to the type mass and propelling it toward the paper to make an imprint. The interposer prevents the hammer from penetrating between adjacent type elements that are moving rapidly in the direction perpendicular to the hammer motion. Upon receiving the momentum from the interposer, the type spends only a fraction of its kinetic energy in printing and returns to the interposer at a relatively high speed. It forcibly impacts the interposer and bounces out again toward the paper. An excessive rebound causes a second imprint on the paper, resulting in "shadow printing."

A damper ring located below the hammer is designed to absorb the impact energy of the returning type and to prevent excessive rebound. It is part of the print disk assem-

Copyright 1979 by International Business Machines Corporation. Copying is permitted without payment of royalty provided that (1) each reproduction is done without alteration and (2) the *Journal* reference and IBM copyright notice are included on the first page. The title and abstract may be used without further permission in computer-based and other information-service systems. Permission to *republish* other excerpts should be obtained from the Editor.

bly and rotates with the interposer and type disks. Note that each interposer finger is firmly in contact with the damper ring; but on impact by the hammer, it is free to move forward to push the type. The striking of the interposer by the returning type mass causes bending of the damper ring, which initiates a flexural wave to propagate and dissipate the impact energy. Attempts to dampen the impact energy with polymers have been unsuccessful, mainly because of the stringent requirements on momentum transmissibility, dimensional stability, and limited motion of the interposers.

Qualitatively, it can be seen that too flexible a damper ring would be as ineffective in damping as would be too massive a damper ring. In these extreme cases, the spring effects of the interposer would become too dominant. Thus, although using the damper ring is intuitively correct, its effectiveness is obtained only through extensive efforts in analysis and experiments.

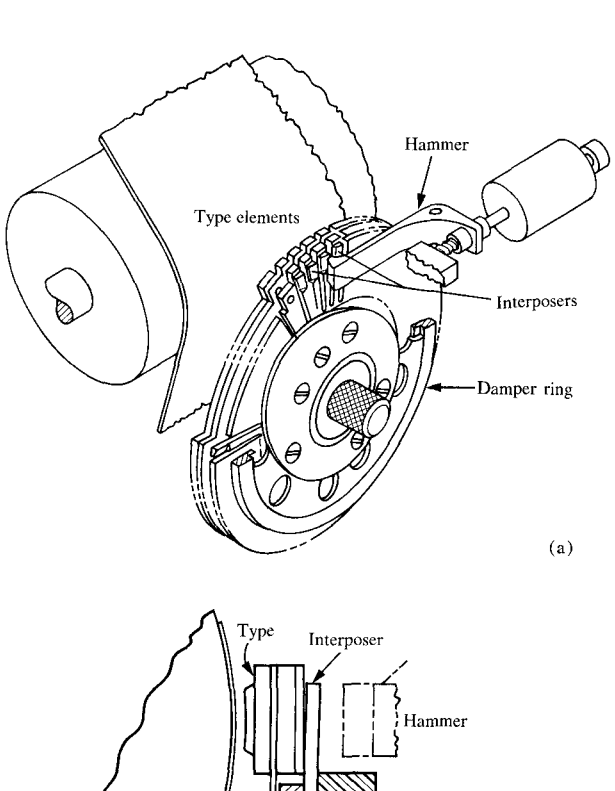
This paper presents the analysis related to the damper design by means of flexural propagation. To simplify the model and generalize it for wider application, the damper ring is taken to be straight and infinitely long; and analyses are made for a mass impacting the beam. Also ignored in the analyses are the small effects due to the disk rotation and the elastic foundation of the circular plate which supports the ring. These simplifications are justified because the peripheral speed of eight meters per second induces a low hoop stress of about 4×10^5 Pa (60 psi) and the supporting plate is sufficiently thin and has ample cutouts to allow the ring to behave like a support-free beam.

Three cases are presented:

- A mass directly impacting the beam. This simplest model gives insight into the damping mechanism of the infinite beam.
- A mass impacting the beam through a linear spring.
 This spring simulates any structural flexibility existing between the mass and the beam, including the contact stress effect.
- 3. A mass impacting a spring that is in parallel with the beam damper. This is a slight variation of the first model and simulates the case where the impacting mass is relatively large compared with the beam, and the additional spring element is needed to approximate the supporting structure.

Analysis

• Dynamic response of the infinite beam We first seek a beam response to an arbitrary load concentrated at x = 0. Noting the symmetry about the origin,



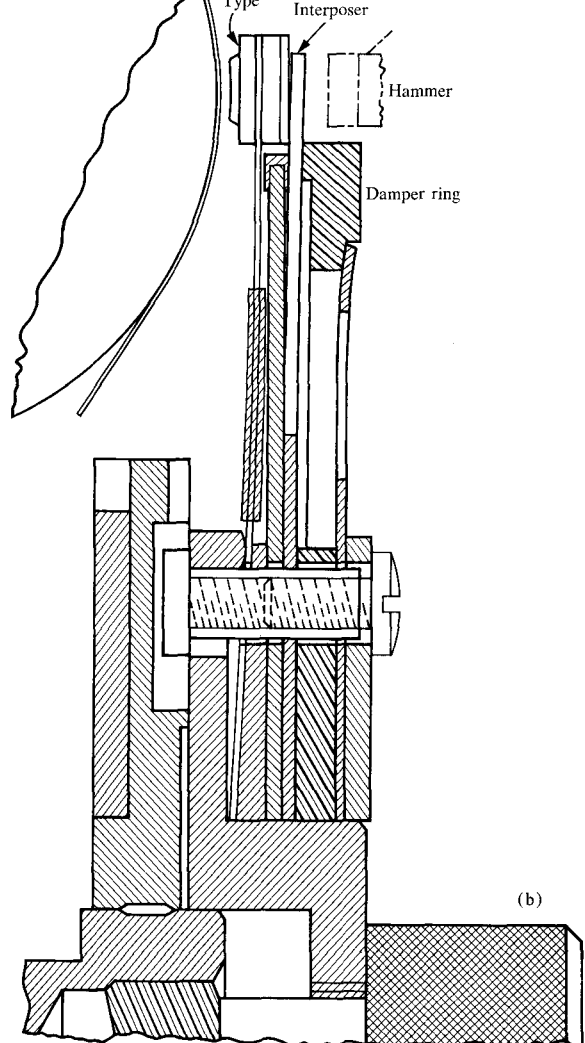


Figure 1 Disk printer. (a) Overall view of disk printer mechanism. (b) Cross section side view of printer disk.

387

the beam equation and boundary and initial conditions are

$$EIw_{xxx} + \rho Aw_{tt} = 0 \qquad x, t > 0, \tag{1}$$

$$w(x, 0) = w_t(x, 0) = 0, (2)$$

$$w_{r}(0,t)=0, (3)$$

$$w_{xxx}(0, t) = \frac{-F(t)}{2EI} , \qquad (4)$$

$$w = w_x = w_{xx} = w_{xxx} = 0$$
 at $x = \infty$, (5)

where EI is the beam modulus, w is the displacement of the beam, ρA is the sectional density, x and t are the space and time coordinates, respectively, F(t) is the concentrated load, and the subscripts designate partial derivatives. We perform the Fourier cosine transform on the above equations, resulting in

$$\bar{w}_{tt}(\alpha, t) + \beta^2 \alpha^4 \bar{w}(\alpha, t) = \frac{F(t)}{2\rho A}, \qquad (6)$$

where

$$\bar{w}(\alpha, t) = \int_0^\infty w(x, t) \cos \alpha x dx, \tag{7}$$

$$\beta^2 = \frac{EI}{\rho A}.\tag{8}$$

Thus.

$$\bar{w}(\alpha, t) = \frac{1}{\beta \alpha^2} \int_0^t \frac{F(\tau)}{2\rho A} \sin \beta \alpha^2 (t - \tau) d\tau, \tag{9}$$

or

$$\bar{w}_t(\alpha, t) = \int_0^t \frac{F(\tau)}{2\rho A} \cos \beta \alpha^2 (t - \tau) d\tau. \tag{10}$$

Now, for the solution, we take the inverse cosine transform of Eq. (10),

$$w_{t}(x, t) = \frac{2}{\pi} \int_{0}^{\infty} \bar{w}_{t}(\alpha, t) \cos \alpha x d\alpha$$

$$= \frac{1}{\pi \rho A} \int_{0}^{t} F(\tau) \int_{0}^{\infty} \cos \alpha x \cos \beta \alpha^{2} (t - \tau) d\alpha d\tau,$$
(11)

and by carrying out the last integration [2],

$$w_t(x, t) =$$

$$\gamma \int_0^t \frac{F(\tau)}{\sqrt{t = \tau}} \left[\cos \frac{x^2}{4\beta(t - \tau)} + \sin \frac{x^2}{4\beta(t - \tau)} \right] d\tau, (12)$$

where

$$\gamma = \frac{1}{\sqrt{8\pi\beta\rho A}} \ .$$

388 At x = 0,

$$w_t(0, t) = \dot{w} = \gamma \int_0^t \frac{F(\tau)}{\sqrt{t - \tau}} d\tau.$$
 (13)

The dot indicates a time derivative when the function is only time dependent. Thus, Eq. (13) gives the beam response in terms of the velocity at the point where the force is applied. For example, if $F(t) = F_0 = \text{constant}$,

$$\dot{w} = 2\gamma F_0 \sqrt{t} . \tag{14}$$

In contrast to a linear dashpot that results in a constant velocity for a constant force, an infinite beam has velocity proportional to \sqrt{t} under a constant force. In another example, if $F = F_0/\sqrt{t}$,

$$\dot{w} = \pi \beta \gamma F_0 = \text{constant}.$$
 (15)

This agrees with Boussnesque's result [3], indicating that constant velocity can be maintained by a force inversely proportional to \sqrt{t} .

• Impact analyses

Case 1

For the first model, we take the simplest case, where the mass m impacts directly on the beam with the initial velocity v_0 and the mass stays with the beam. Then, in terms of the mass velocity v,

$$m\dot{v} = -F(t),\tag{16}$$

$$v = \gamma \int_0^t \frac{F(\tau)}{\sqrt{t - \tau}} d\tau = -m\gamma \int_0^t \frac{\dot{v}(\tau)}{\sqrt{t - \tau}} d\tau.$$
 (17)

The Laplace transform of Eq. (17) gives

$$V(s) = \frac{v_0}{\sqrt{s} \left(\sqrt{s} + \frac{1}{m\gamma\sqrt{\pi}}\right)},$$
 (18)

and, therefore,

$$v(t) = v_0 e^{\frac{t}{\pi m^2 \gamma^2}} \operatorname{erfc}\left(\frac{\sqrt{t}}{m_0 \sqrt{\pi}}\right), \tag{19}$$

where erfc is the complementary error function.

Again, compared to a linear dashpot for which the velocity of the impacting mass decays exponentially, the velocity of the mass impacting an infinite beam decays more slowly for large t. As a matter of fact, Eq. (19) shows v decreasing as a function of $1/\sqrt{t}$ for large t.

Case 2

Next, we consider a case where the mass impacts the beam through a spring. This is analogous to the Maxwell model shown in Fig. 2. As the impacting mass compresses the spring, the extent of the rebound of the mass

depends on the inertia and rigidity of the beam. Our interest lies in the range where rebound occurs. The equations of motion are

$$m\ddot{y} = -F(t) = -k(y - w) = -kz,$$
 (20)

$$\dot{w} = \gamma \int_0^t \frac{F(\tau)}{\sqrt{t - \tau}} d\tau = -k\gamma \int_0^t \frac{z(\tau)}{\sqrt{t - \tau}} d\tau, \tag{21}$$

where y and w denote the displacements of the mass and the beam, respectively, and z is their relative displacement. Set

$$\eta = \omega t, \tag{22}$$

$$\omega^2 = \frac{k}{m} \,, \tag{23}$$

and

$$\tilde{\alpha} = m\gamma \sqrt{\omega} = \frac{1}{\sqrt{8\pi}} \left[\frac{m^3 k}{EI(\rho A)^3} \right]^{1/4}$$
 (24)

Then, Eqs. (20) and (21) become

$$w''(\eta) = -(z'' + z), \tag{25}$$

$$w' = \tilde{\alpha} \int_0^{\eta} \frac{z(\xi)}{\sqrt{\eta - \xi}} d\xi. \tag{26}$$

The primes denote the derivatives with respect to the independent variable. Taking, again, the Laplace transforms of Eqs. (25) and (26), and solving for Z,

$$\frac{Z(s)}{\tilde{V}_0} = \frac{1}{s^2 + \tilde{\alpha}\sqrt{\pi s} + 1} = \frac{s^2 + 1 - \tilde{\alpha}\sqrt{\pi s}}{s^2 + 1 - \pi\tilde{\alpha}^2 s}, \quad (27)$$

where $\bar{V}_0 = \dot{y}(0)/\omega$. The inverse transform of the above equation involves finding the roots of the denominator, which are in the form of $p \pm iq$, $-p \pm ir$. Using partial fractions for the final solution results in

$$\frac{z(\eta)}{\bar{V}_0} = e^{p\eta} \left(A_1 \cos q\eta + \frac{B_1}{q} \sin q\eta \right)
+ e^{-p\eta} \left(C_1 \cos r\eta + \frac{D_1}{r} \sin r\eta \right)
- \bar{\alpha} \int_0^{\eta} \frac{1}{\sqrt{\xi}} \left\{ e^{p(\eta - \xi)} \left[A_2 \cos q(\eta - \xi) \right]
+ \frac{B_2}{q} \sin q(\eta - \xi) \right]
+ e^{-p(\eta - \xi)} \left[C_2 \cos r(\eta - \xi) \right]
+ \frac{D_2}{r} \sin r(\eta - \xi) \right\} d\xi.$$
(28)

The constants A_1 , A_2 , B_1 , \cdots , D_2 are obtained through

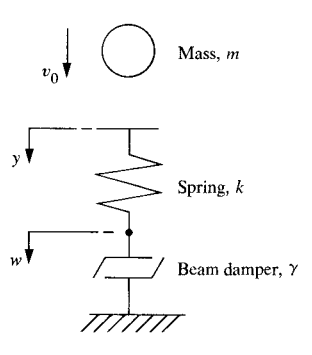


Figure 2 Model for Case 2 (Maxwell model).

partial fractions which yield simultaneous equations. The equations in a matrix form are

$$\begin{bmatrix} 1 & 0 & 1 & 0 \\ p & 1 & -p & 1 \\ (r^2 - p^2) & 2p & (q^2 - p^2) & -2p \\ -p(p^2 + r^2) & (p^2 + r^2) & p(r^2 + q^2) & 2(p^2 + q^2) \end{bmatrix} \begin{bmatrix} A \\ B \\ C \\ D \end{bmatrix}$$

For A_1 , B_1 , C_1 and D_1 , \bar{N} is (0 1 0 1); for A_2 , B_2 , C_2 and D_2 , \bar{N} takes the form (0 0 1 0).

The velocity is computed from Eq. (20),

$$y'(\eta) = 1 - \int_0^{\eta} z(\xi) d\xi.$$
 (29)

The integrations in Eqs. (28) and (29) may be performed numerically. The square root singularity in Eq. (28) can be eliminated by a variable substitution, $\varphi = \sqrt{\xi}$ or $d\varphi = d\xi/\sqrt{\xi}$.

The rebound velocity is the velocity y' when the relative displacement z becomes zero (at $\eta = \eta_c$). Then the coefficient of restitution, the ratio of rebound velocity to the initial velocity, is

$$R = \int_0^{\eta_c} z(\xi)d\xi - 1, \tag{30}$$

where $z(\eta_c) = 0$. Note that in this analysis there is only one parameter, $\tilde{\alpha}$, which is defined by Eq. (24). Thus, the rebound characteristics of this model are represented by a single curve, as shown in Fig. 3, which indicates there is no rebound for $\tilde{\alpha}$ greater than about 0.52.

Case 3

Case 2 represents the situation where a small mass impacts a relatively massive beam. There, the supporting structure of the beam can be ignored. However, as the beam is made lighter compared to the impacting mass, the rebounding characteristics are dictated more by the elas-

389

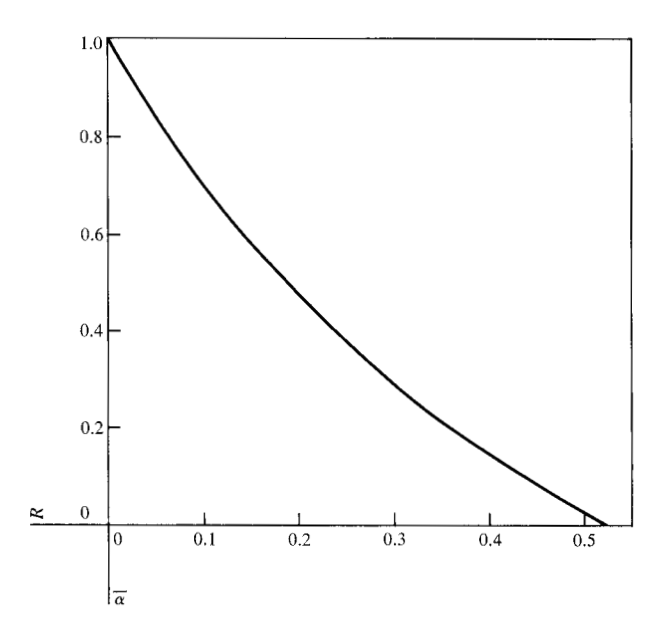


Figure 3 Coefficient of restitution (R) vs $\bar{\alpha}$ for Case 2.

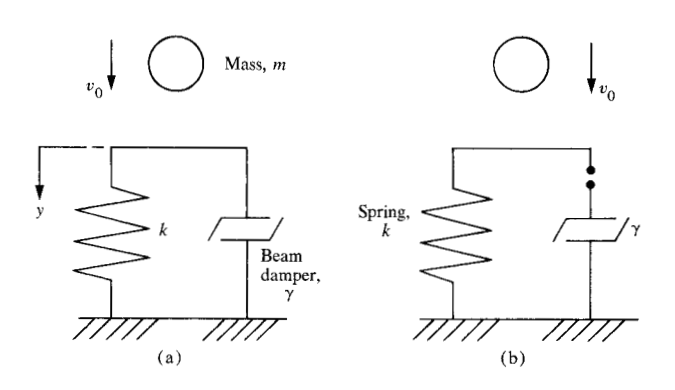


Figure 4 Model for Case 3 (Kelvin-Voigt model). Type (a): Spring and beam tied together. Type (b): Spring can push beam downward but cannot pull it up.

ticity of other supports. We represent such elasticity by a spring that acts in parallel to the beam as shown in Fig. 4 and is known as the Kelvin-Voigt type. Two different types may be studied for this model: one in which the spring and the beam are tied together, Fig. 4(a), and another in which the spring can push the beam downward but cannot pull it up, Fig. 4(b).

When the mass impacts the spring, it pushes the beam until the maximum deflection is reached. At this point, for the second type of the model, the spring can separate from the beam, transforming the spring energy into kinetic energy of the mass. On the other hand, for the type in which the spring and the beam are tied together, the

spring pulls the mass and the beam until the maximum upward velocity is reached, at which point the separation occurs. For this model the equations of motion for both Figs. 4(a) and 4(b) are

$$m\ddot{y} = -ky - F(t), \tag{31}$$

$$\dot{y} = \gamma \int_0^t \frac{F(\tau)}{\sqrt{t - \tau}} d\tau. \tag{32}$$

If we combine the two equations, substitute $\eta = \omega t$ and take the Laplace transform, we get

$$\frac{Y(s)}{\bar{V}_0} = \frac{1}{s^2 + \frac{1}{\sqrt{\pi}\,\bar{\alpha}}} \sqrt{s^3 + 1}$$

$$= \frac{s^2 + 1 - \frac{1}{\sqrt{\pi}\,\bar{\alpha}}}{(s^2 + 1)^2 - \frac{1}{\pi\bar{\alpha}^2}} s^3$$
(33)

and

$$\frac{V(s)}{\bar{V}_0} = \frac{s}{s^2 + \frac{1}{\sqrt{\pi}\,\bar{\alpha}}} \sqrt{s^3 + 1} \ . \tag{34}$$

This method of solution is similar to that in Case 2, with the solution again depending on only one parameter, $\tilde{\alpha}$. The restitution as a function of $\tilde{\alpha}$ is plotted in Fig. 5 for both types.

• Application to beam damper design

The curves in Figs. 3 and 5, which summarize the preceding analysis, can provide very useful information for a damper design. All the physical parameters of the beam, the mass, and the spring are conveniently lumped into one parameter $\tilde{\alpha}$, as defined by Eq. (24). Thus, many different combinations of parameters can result in a desirable value of $\tilde{\alpha}$. One has only to decide which curve in Figs. 3 or 5 best models one's damper system. Then, with the value of $\tilde{\alpha}$ known, one can obtain the expected rebound characteristics of the damper.

In the case of the disk printer described earlier, early poor settle-out and shadow printing were attributed to too light a damper ring made of nylon. The interposer flexibility was the dominant factor for the rebound simulating Case 3 [Fig. 4(b)], with a high value of $\tilde{\alpha}$ (about 2.5). To decrease the value of $\tilde{\alpha}$, a material with high density was sought to increase the value ρA , the most influential factor in altering the value of $\tilde{\alpha}$, as seen in Eq. (24). A tungsten-filled nylon was selected and the maximum area A that the space allowed was filled. The final modification was successful in eliminating the shadow printing; the

value of $\tilde{\alpha}$ was sufficiently lowered to about 0.4, which fell in the range of Case 2.

Summary

Dynamic response of an infinite beam is used to analyze the flexural wave propagation as a means of dissipating impact energy. A simple form of the basic response to arbitrary loading is derived, and the damping characteristics of the beam are analyzed through impacts between a mass and the beam, with springs arranged as in the Maxwell and Kelvin-Voigt models. The results are summarized in simple curves with a single lumped parameter that combines the physical parameters of the mass, the beam, and the spring. These curves provide useful information for the design of beam dampers.

References

- 1. J. H. Meier and J. W. Raider, "Interposer for Disk Printer," *IBM J. Res. Develop.* 23, No. 4, 392-395 (1979, this issue).
- L. Meirovitch, Analytical Methods in Vibrations, The Macmillan Co., New York, 1967, Ch. 8, pp. 356-362.
- P. E. Duwez, D. C. Clark, and H. F. Bohnenblust, "The Behavior of Long Beams Under Impact Loading," J. Appl. Mech. 17, No. 1, 27-34 (1950).

Received December 4, 1978; revised February 12, 1979

H. C. Lee is located at the IBM System Products Division laboratory, P.O. Box 6, Endicott, New York 13760; J. W.

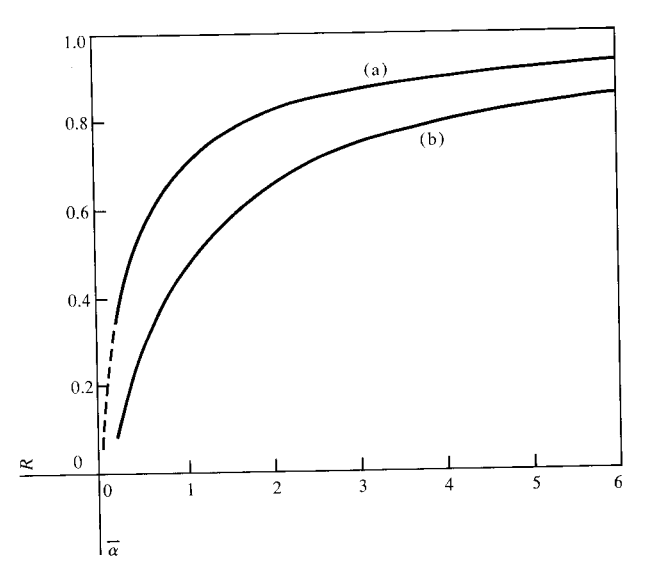


Figure 5 Coefficient of restitution (R) $vs \tilde{\alpha}$ for Case 3.

Raider is located at the IBM Office Products Division laboratory, Lexington, Kentucky 40507.